Electro-mechanical analysis of flexural transducers

Andrew Feeney, Lei Kang, George Rowlands, and Steve Dixon
Centre for Industrial Ultrasonics, Department of Physics, University of Warwick, Coventry UK
a.feeney@warwick.ac.uk

EPSRC Engineering and Physical Sciences Research Council

1. Flexural transducers

The flexural transducer, shown in Figure 1, is an ultrasonic device comprising a piezoelectric ceramic bonded to a metal cap, often titanium or aluminium. The metallic membrane constrains the piezoelectric ceramic, whose vibration produces a bending motion of the membrane, thereby generating the required ultrasound.

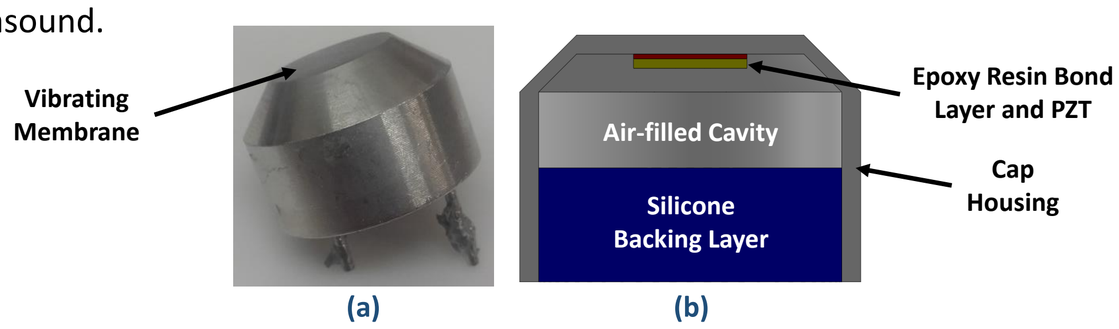

Figure 1: (a) An aluminium-capped flexural transducer, and (b) the assembly schematic (not to scale), for a flexural transducer.

The efficiency of a flexural transducer is dependent on the membrane bending, not by impedance mismatch like a bulk piezoelectric. This makes them attractive candidates for wetted transducers. Flexural transducers are used in a range of applications including robotics, NDT inspection, material characterisation, as parking sensors, and in flow metering. Different applications may require multiple frequencies, which can be controlled through manipulation of the membrane layer material and dimensions. Two common axisymmetric modes of vibration are shown in Figure 2.

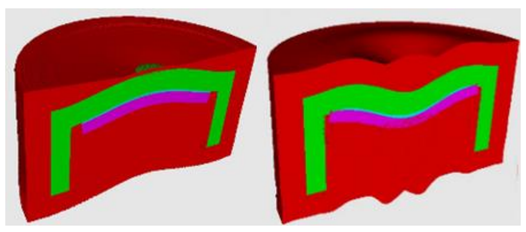

Figure 2: Modes of vibration of a flexural transducer, showing (a) the (0,0) mode, and (b) the (1,0) mode, simulated with PZFlex® finite element analysis software. The red regions denotes a simulated air environment.

2. Characterisation techniques

Experimental techniques for investigating the response of flexural transducers include the use of acoustic microphones and laser Doppler vibrometry. Figure 3 shows a suitable experimental set-up, and an example of rapid resonance frequency measurement using just a function generator and oscilloscope.

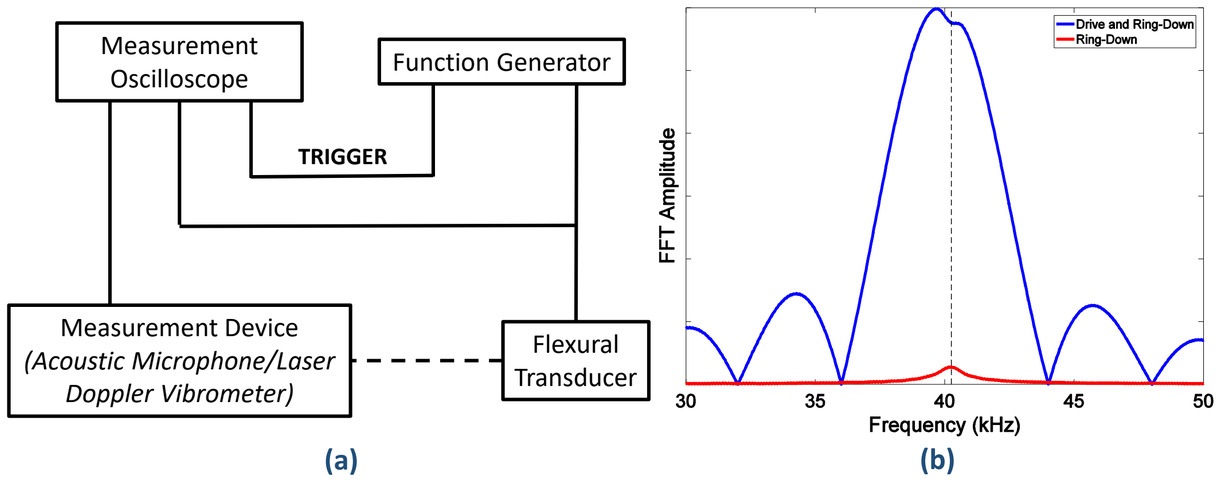

Figure 3: (a) Experimental set-up for the characterisation of flexural transducers, and (b) FFT of transducer response showing measurement of resonance at 40 kHz.

3. Resonance frequency measurement

The response of the flexural transducer for a drive excitation frequency of 45 kHz is shown in Figure 4. The response has been measured using laser Doppler vibrometry. When the drive signal is switched on, the transducer membrane oscillates at varying amplitude before reaching a steady-state amplitude. When the drive signal is switched off, the transducer membrane almost immediately vibrates at resonance, shown by the inset figure.

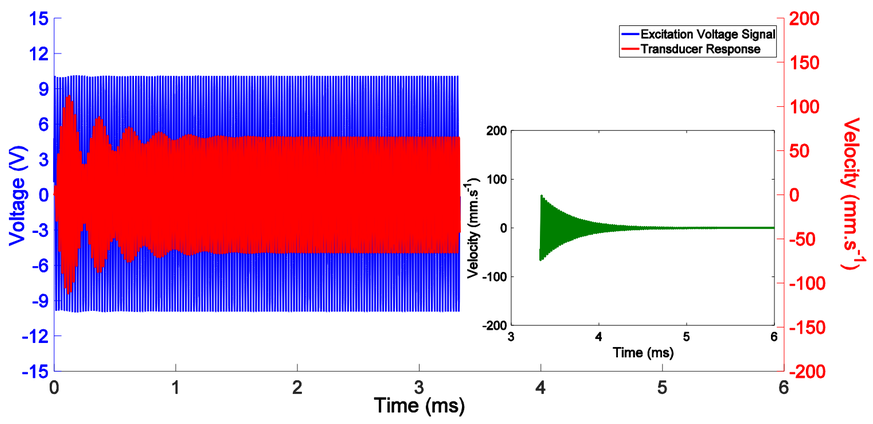

Figure 4: Flexural transducer response for a 45 kHz drive frequency, where the inset shows decay at resonance after drive signal is switched off.

4. Transducer characterisation

The flexural transducer can be operated over a range of drive excitation frequencies. Measurement of the amplitude velocity of the transducer membrane at each of these frequencies using laser Doppler vibrometry enables the amplitude and resonance behaviour to be determined, as shown in Figure 5. Through a zero-crossing method, the effective frequency response over time can be computed, as displayed in Figure 6. When the drive is switched off, the transducer instantly vibrates at its resonance frequency.

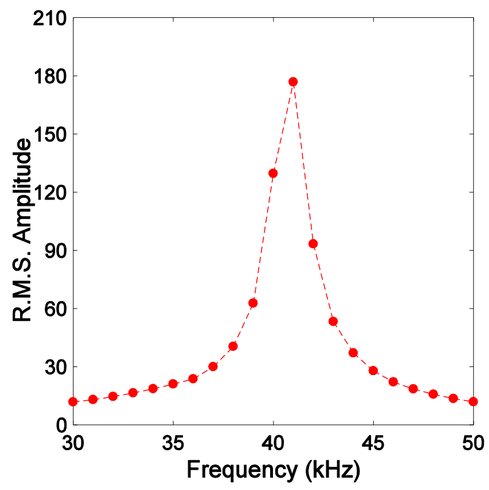

Figure 5: Amplitude-frequency response at different excitation frequencies.

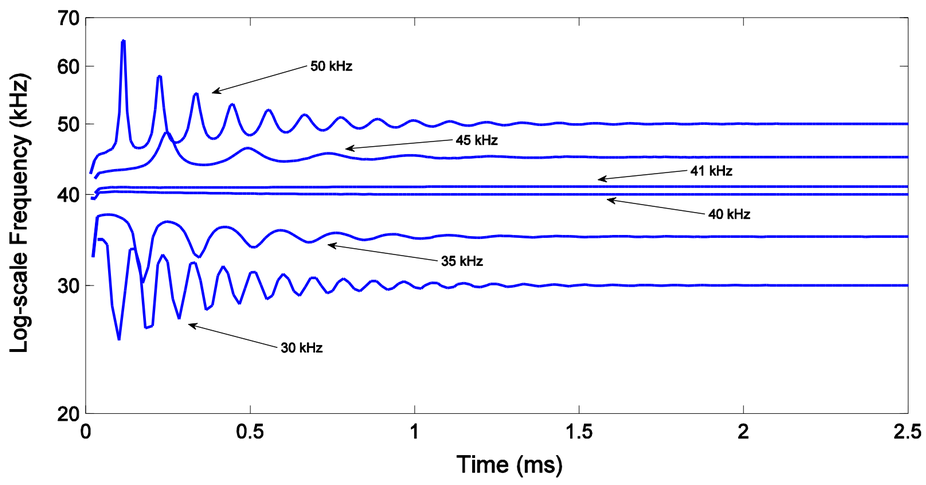

Figure 6: Effective frequency response at different excitation frequencies.

5. Mathematical analogue

A mathematical analogue for the flexural transducer is shown in Figure 7, with a sample spectrum detailing the response regions. Equations of motion for the regions are provided in Equations (1) to (3), with mass, M, damping, C, and stiffness K, angular frequency, ω and time, t.

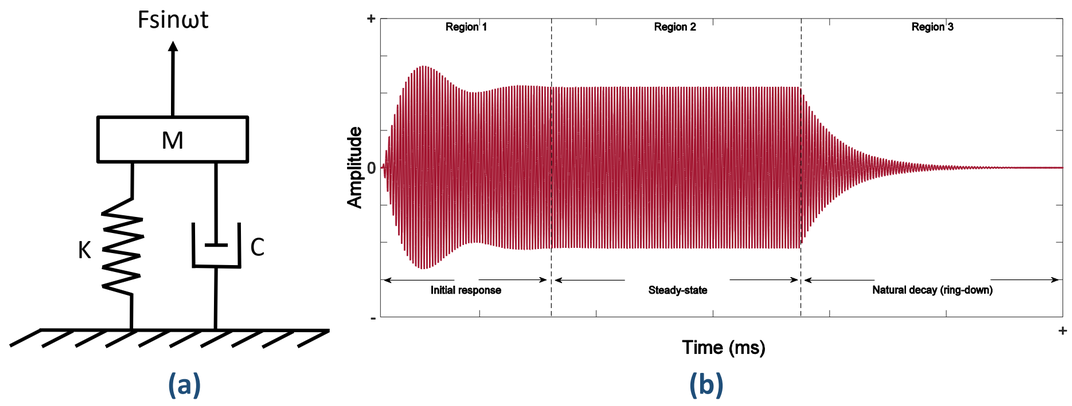

Figure 7: (a) The mathematical analogue model, and (b) the response regions.

Region 1 $M\ddot{x} + C\dot{x} + Kx = Fsin\omega t.H(t_0 - t)$ **Equation (1)**

Region 2 $M\ddot{x} + C\dot{x} + Kx = Fsin\omega t$ **Equation (2)**

Region 3 $M\ddot{x} + C\dot{x} + Kx = 0$ **Equation (3)**

Regions 2 and 3 designate steady-state and natural decay, and Region 1 is a convolution of a sinusoidal wave with a Heaviside step function, which can also be considered as a superposition of two signals, the decaying resonance and the drive, according to the solution shown in Equation (4). Experimental and simulation results using this method are compared in Figure 8.

$$x(t) = Asin(\omega t - \theta) + Be^{-\frac{C}{2M}}sin(\omega_n t - \Phi) \quad \textbf{Equation (4)}$$

A and B are the amplitudes of the drive and resonance signals respectively, θ and Φ denote the drive and resonance signal phases, ω indicates the angular drive frequency, and ω_n represents the angular resonance frequency.

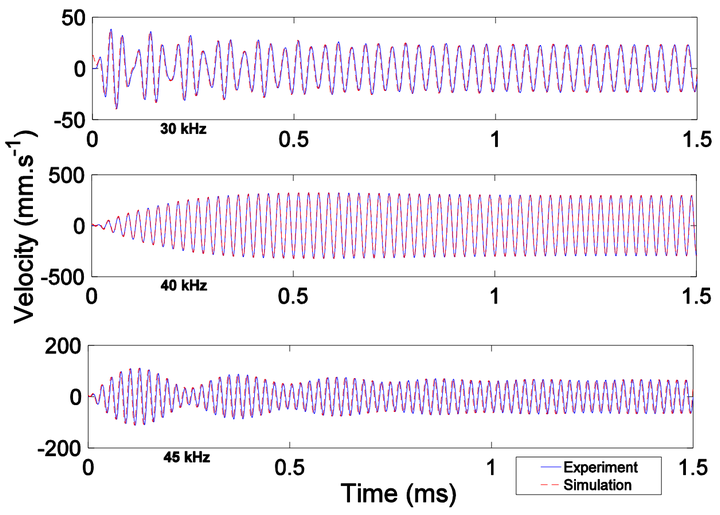

Figure 8: Experimental and simulation results for three drive frequencies.

Acknowledgements
Michael Ginestier and Christopher Wells are acknowledged for their contributions to this research.
This research is funded by the EPSRC, Grant No. EP/N025393/1.